Supplement of Atmos. Chem. Phys., 24, 6987–6999, 2024
https://doi.org/10.5194/acp-24-6987-2024-supplement

Atmospheric Chemistry and Physics Open Access

Supplement of

Different formation pathways of nitrogen-containing organic compounds in aerosols and fog water in northern China

Wei Sun et al.

Correspondence to: Guohua Zhang (zhanggh@gig.ac.cn) and Xinhui Bi (bixh@gig.ac.cn)

Text S1. The solid-phase extraction operation

For FT-ICR MS analysis, water-soluble organic compounds in fog water and aerosols extract were isolated using solid-phase extraction (SPE). The SPE cartridges (Strata-X, Phenomenex, USA) were pre-conditioned sequentially with 3 mL of isopropanol, 6 mL of acetonitrile, 6 mL of methanol containing 0.1% of formic acid, and 6 mL of ultrapure water containing 0.1% formic acid. Then, 10 mL of fog water and aerosols extracts with pH adjusted to 4.5 using formic acid were added to the cartridge at a flow rate of approximately 1 mL min^{-1}. The inorganic salts were removed from the cartridge using 4 mL of ultrapure water containing 0.1% formic acid. Note that some low-weight organic molecules are expected to be lost in this step. The cartridges were then freeze-dried, and the analytes were eluted using 3 mL of acetonitrile / methanol / ultrapure water (45 / 45 / 10, *v:v:v*) at pH 10.4, with the pH being adjusted using ammonium hydroxide. All the solvents were HPLC-grade. Blank samples of the fog water and aerosols were processed and analyzed following the same procedure as the samples.

Text S2. Instrumental analysis of FT-ICR MS

A solariX XR FT-ICR MS instrument (Bruker Daltonik GmbH, Bremen, Germany) equipped with a 9.4-T refrigerated, actively shielded superconducting magnet (Bruker Biospin, Wissembourg, France) and a Paracell analyzer cell was used for the analysis in this study. An electrospray ionization (ESI) source (Bruker Daltonik GmbH, Bremen, Germany) in both negative and positive ionization modes (ESI− and ESI+) was used to ionize the organics. The samples were redissolved in 1 mL of methanol and injected into the ESI source at a flow rate of 200 μL h^{-1}. A nebulizer gas pressure of 1 bar, a dry gas velocity of 4 L min^{-1} and temperature of 200°C, and capillary voltages of +/− 4500 V (+4500 and −4500 were used for ESI− and ESI+, respectively) and the end plate offset −500 V were used for ESI source. An argon-filled hexapole collision pool was operated at 2 MHz and 1400 Vp-p RF amplitude. The time of flight was 0.7 ms and the ion accumulation time was 0.1 s. A total of 128 continuous 4M data FT-ICR transients were co-added to enhance the signal-to-noise ratio and dynamic range. A typical mass-resolving power (m/Δm50%, where Δm50% is the magnitude of the mass spectral peak full width at half-maximum peak height) of more than 450,000 at m/z 319 with <0.3 ppm absolute mass error was achieved. The final spectrum was internally calibrated with typical class species peaks in samples using quadratic calibration in DataAnalysis 5.0 (Bruker Daltonics).

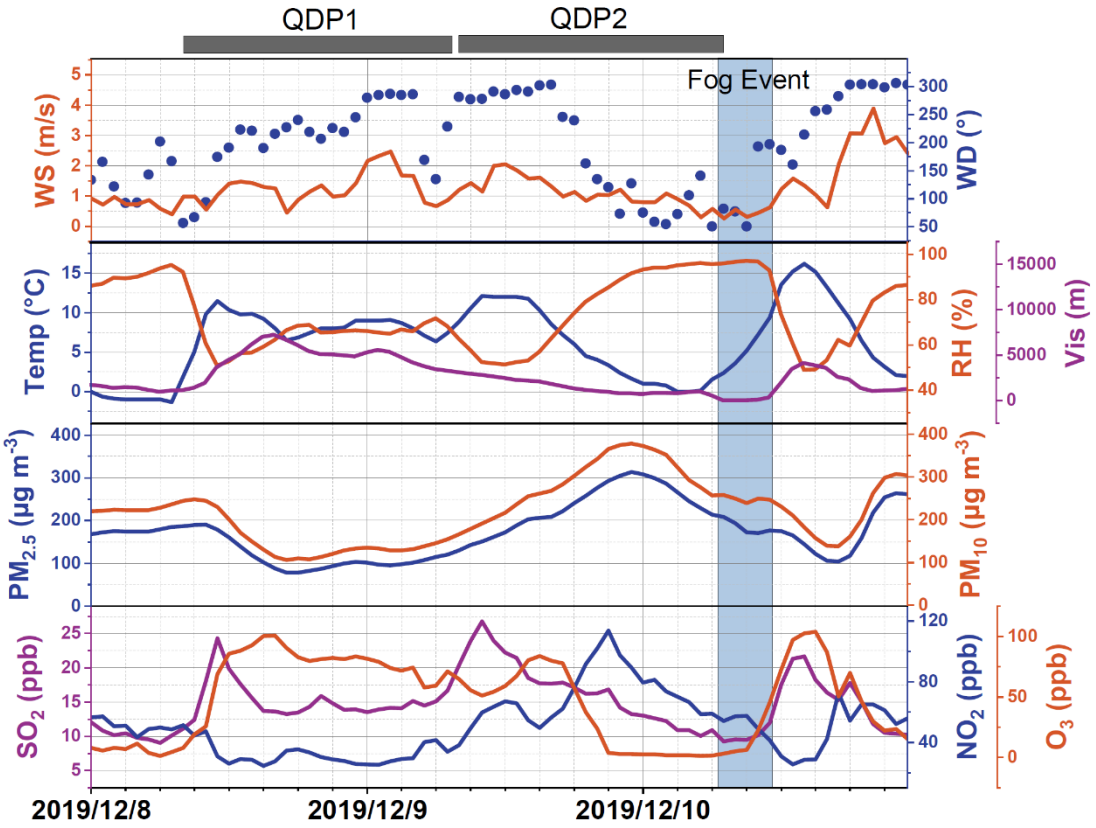

Figure S1. The detailed temporal variations of meteorological and pollution conditions during the sampling. The grey boxes above the plots represent the starting and ending time of the aerosol sampling. The blue shadow represents the time period of fog event.

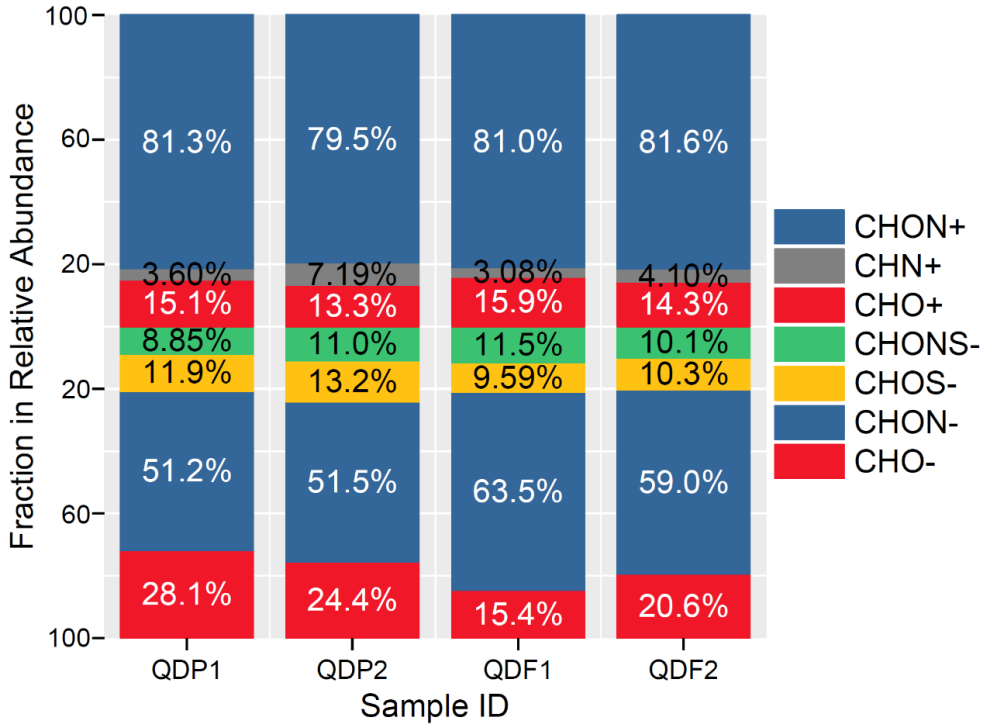

Figure S2. The fraction in relative abundance (%) of the four groups (CHO−, CHON−, CHOS−, and CHONS−) in ESI− mode and three groups (CHO+, CHON+, and CHN+) in ESI+ mode.

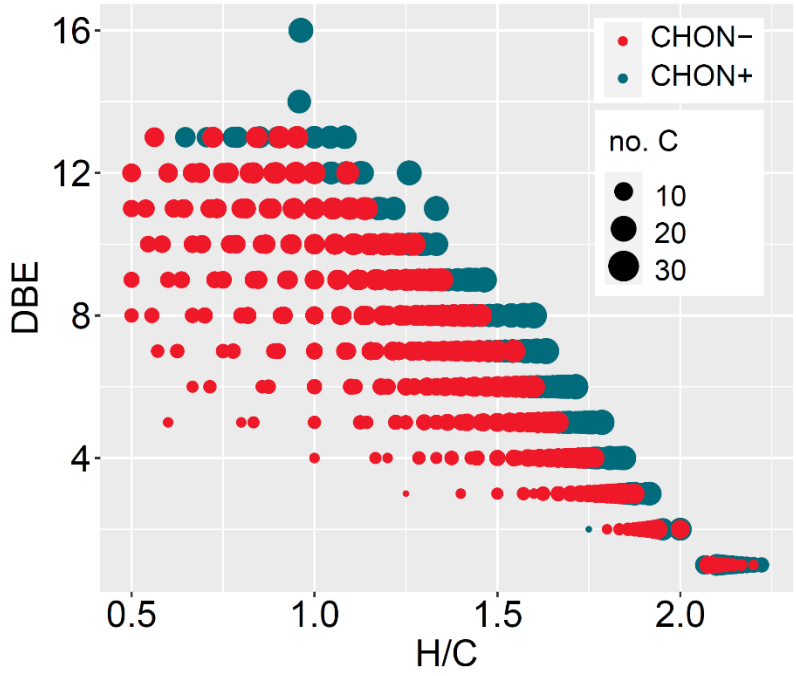

Figure S3. The plot of DBE versus H/C ratios in pre-fog aerosol sample QDP1. no. C in the plot represents the number of carbon atoms in NOC molecules.

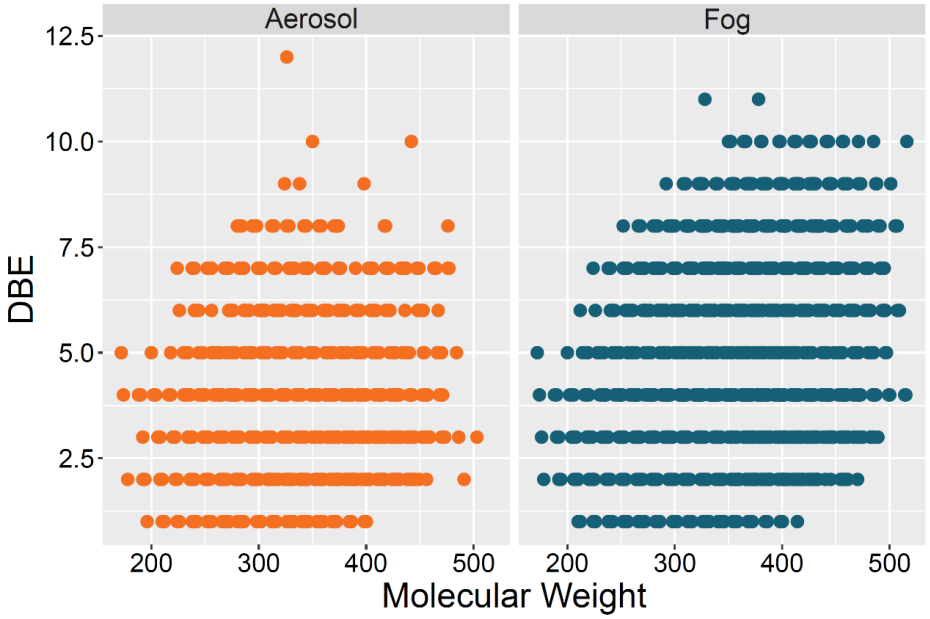

Figure S4. The plot of DBE versus molecular weight of $CHONS^-$ in aerosols and fog water.

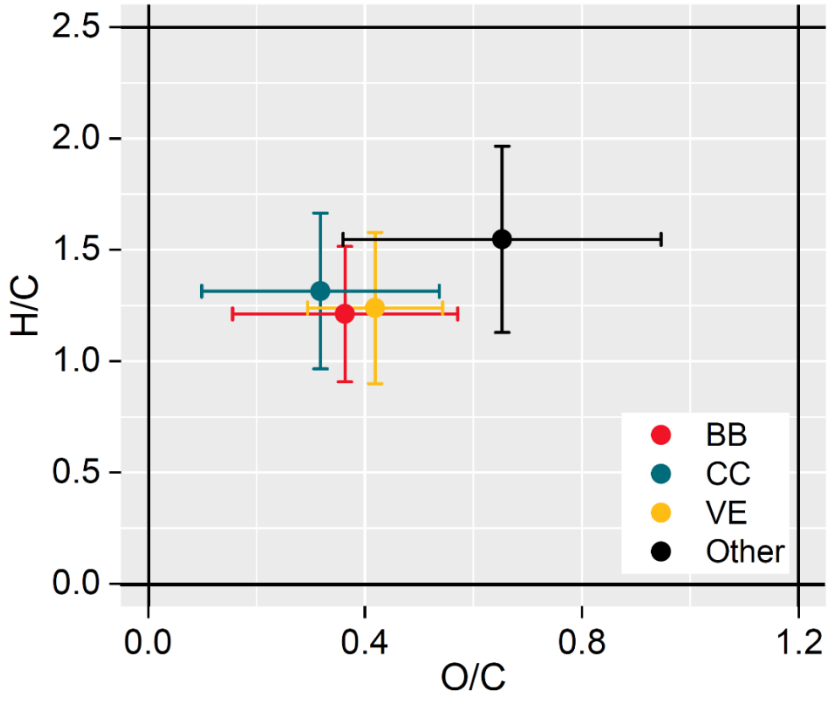

Figure S5. The Van Krevelen diagram for NOCs from different sources (biomass burning, BB; coal combustion, CC; vehicle emission, VE; and other sources) in pre-fog aerosols. The dots in the plot represent the average values of O/C and H/C, and the error bars represent standard deviation.

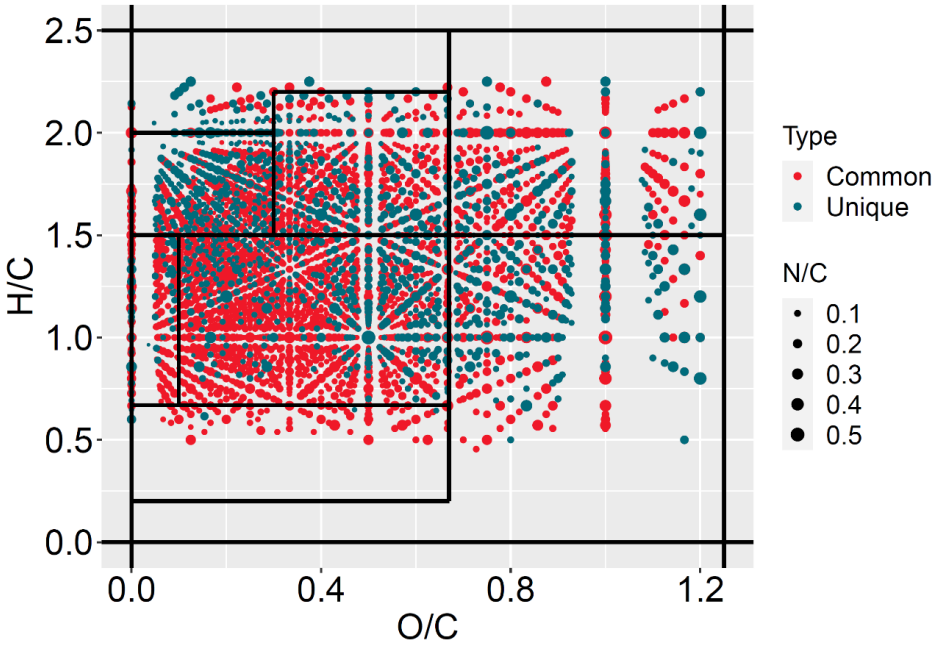

Figure S6. The Van Krevelen diagram for common and unique NOC molecules in fog water compared with pre-fog aerosols.

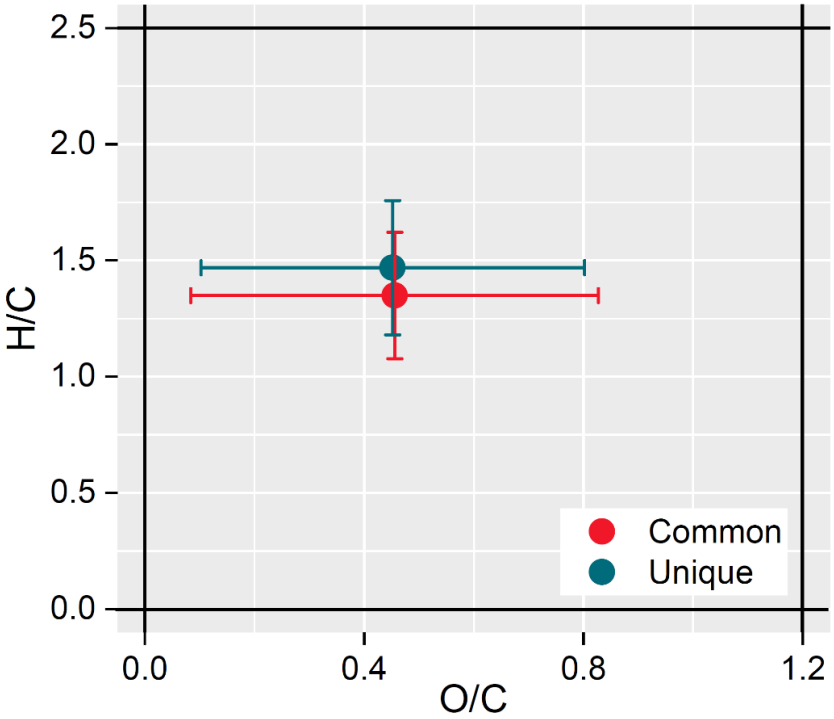

Figure S7. The Van Krevelen diagram for common and unique NOC molecules in fog water compared with pre-fog aerosols. The dots in the plot represent the average values of O/C and H/C, and the error bars represent standard deviation.

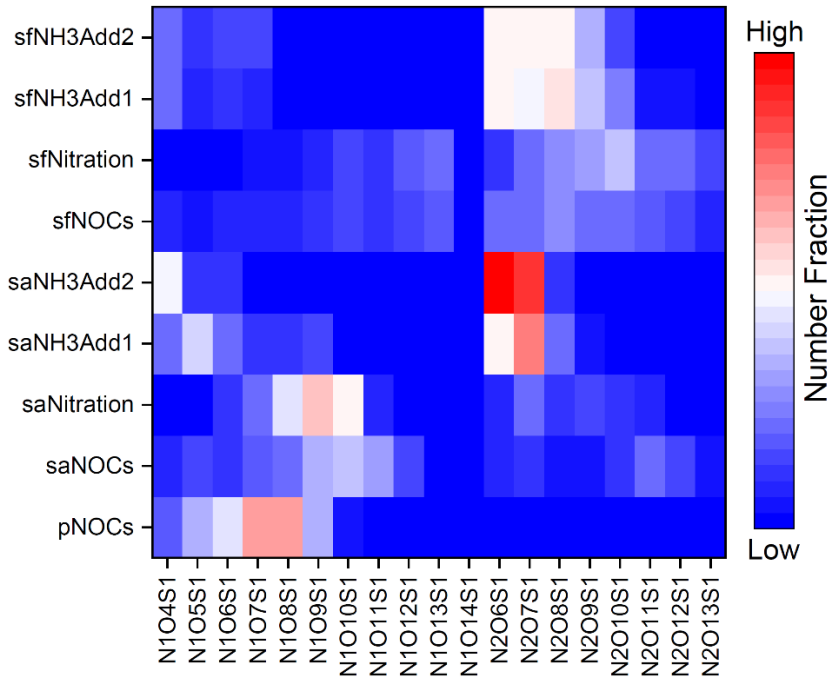

Figure S8. The heat map of subclasses of CHONS divided by the number of N, O, and S atoms in pNOCs, saNOCs, and sfNOCs.

Table S1. The reactions considered in the "precursor–product pair" analysis.

Reaction Type	Transformation Reaction	Variation of Atoms
Dealkyl group	demethylation	−CH2
Dealkyl group	Di-demethy or Deethylation	−C2H4
Dealkyl group	Deisopropyl	−C3H6
Dealkyl group	Dealkylation	−C2H2
Oxygen addition	Hydroxylation/N or S-oxidation	+O
Oxygen addition	Carbonylation/Methyl to aldehyde/Alcohol to carboxylic acid/Primary amine to nitro	−H2+O
Oxygen addition	Hydration	+H2O
Oxygen addition	Methyl to carboxylic acid	−H2+O2
Oxygen addition	Oxygen addition	+O2
Oxygen addition	Oxygen addition	+O3
Oxygen addition	Oxidation of carbon-carbon double bond	+H2O2
Reaction of carboxylic acid	Decarboxylation	−CO2
Reaction of carboxylic acid	Loss of acetic acid	−C2H2O2
Reaction of carboxylic acid	Reductive displacement of carboxylic acid	−COOH+OH
Reaction of carboxylic acid	Decarboxylation to carbonyl/Loss of aldehyde	−CH2O
Reaction of carboxylic acid	Decarboxylation to peroxide	−C
Reaction of amine	Deamination	−NH
Reaction of amine	Oxydative displacement of amine	−NH2+OH
Reaction of amine	Deamination to ketone	−NH3+O
Reaction of amine	Demethylamine to hydroxy	−CH3NH+OH
Reaction of amine	Oxidation of tertiary amine	−N+HO2
Reaction of amine	deamidization	−CONH+H2
Reaction of amine	Hydrolysis of amide	−CONH+H2O
Reaction of the nitro/nitroso group	Loss of nitro group	−NO2+H
Reaction of the nitro/nitroso group	Nitroso reduction/Reductive displacement of oxygen	−O+H2
Reaction of the nitro/nitroso group	Oxidative displacement of nitro group	−NO2+OH
Reaction of the nitro/nitroso group	Nitration	−H+NO2

Table S1 Continued.

Reaction Type	Transformation Reaction	Variation of Atoms
Reaction of sulfur	Desulfonation	−SO2
Reaction of sulfur	Desulfurization	−S
Reaction of sulfur	Oxidative displacement of sulfhydryl/Oxidative displacement of sulfur	−SH+OH
NH3 addition	Reaction of aldehydes or ketones with ammonia	−O+NH
NH3 addition	Reaction of imine with carbonyls present in the skeleton of the same molecule	−HO2+N
Other reactions	Dehydrogenation	−H2
Other reactions	Hydrogenation	+H2
Other reactions	Loss of oxygen	−O
Other reactions	Dehydration	−H2O
Other reactions	Deacetylation	−C2H2O
Other reactions	Oxidative displacement of methyl to alcohol	−CH2+O
Other reactions	Oxidative displacement of methyl to ketone	−CH4+O

Table S2. The number of products formed by nitration and NH_3 addition reactions in pre-fog aerosols and fog water, the number of that detected by ESI− and ESI+, and the number ratios of that detected by two ionization modes.

		Total Number	Numb. in ESI+	Numb. in ESI−	$MNR_{+/-}$
Pre-Fog Aerosol	Nitration	450	64	407	0.16
	NH3Add1	228	117	137	0.85
	NH3Add2	120	61	80	0.76
Fog Water	Nitration	352	73	290	0.25
	NH3Add1	374	181	215	0.84
	NH3Add2	390	182	233	0.78

Table S3. The criteria for the division of seven categories in the VK plot.

Category	H/C	O/C
Lipid-like	1.5<H/C≤2.0	0≤O/C≤0.3
Aliphatic/peptide-like	1.5<H/C≤2.2	0.3<O/C≤0.67
CRAM-like structures	0.67<H/C≤1.5	0.1≤O/C<0.67
Carbohydrate-like	1.5<H/C≤2.25	0.67<O/C≤1.2
Unsaturated hydrocarbons	0.67<H/C≤1.5	O/C<0.1
Aromatic structures	0.2≤H/C≤0.67	O/C<0.67
Highly Oxygenated Compounds	0.6<H/C≤1.5	0.67≤O/C≤1.2